A malarial cysteine protease is necessary for *Plasmodium* sporozoite egress from oocysts

Ahmed S.I. Aly and Kai Matuschewski

Department of Parasitology, Heidelberg University School of Medicine, 69120 Heidelberg, Germany

The *Plasmodium* life cycle is a sequence of alternating invasive and replicative stages within the vertebrate and invertebrate hosts. How malarial parasites exit their host cells after completion of reproduction remains largely unsolved. Inhibitor studies indicated a role of *Plasmodium* cysteine proteases in merozoite release from host erythrocytes. To validate a vital function of malarial cysteine proteases in active parasite egress, we searched for target genes that can be analyzed functionally by reverse genetics. Herein, we describe a complete arrest of *Plasmodium* sporozoite egress from *Anopheles* midgut oocysts by targeted disruption of a stage-specific cysteine protease. Our findings show that sporozoites exit oocysts by parasite-dependent proteolysis rather than by passive oocyst rupture resulting from parasite growth. We provide genetic proof that malarial cysteine proteases are necessary for egress of invasive stages from their intracellular compartment and propose that similar cysteine protease–dependent mechanisms occur during egress from liver-stage and blood-stage schizonts.

CORRESPONDENCE
Kai Matuschewski:
Kai_Matuschewski@
med.uni-heidelberg.de

Malaria is caused by intracellular parasites of the phylum Apicomplexa that can enter and exit host cells. The characterization of parasite and host cell proteins involved in *Plasmodium* cell entry has provided a detailed understanding of the underlying mechanisms (1) and led to new intervention strategies (2). In contrast, the equally important process of *Plasmodium* release is less well understood. With the exception of ookinetes, invasive stages (i.e., sporozoites, liver-stage merozoites, and blood-stage merozoites) are formed by multiple fission in processes called sporogony and merogony, respectively. These stages then need to egress from their intracellular compartment and, shortly thereafter, from their host cell. Inhibitor studies suggested that multiple proteolytic events occur during rupture of schizont-infected erythrocytes and subsequent reinvasion of erythrocytes (3, 4). Treatment of intracellular schizonts with the cysteine protease inhibitor E64 resulted in accumulation of membrane-enclosed viable merozoites (5, 6). In support of active proteolytic events during parasite egress, stage-specific expression of cysteine and serine protease activities has been detected (7). In addition, several genes that encode potential cysteine proteases have been identified and characterized in *Plasmodium* (8). They include falcipain 1, a nonessential cathepsin L–like cysteine protease with yet undefined functions in oocyst development (9, 10), the food vacuole–resident hemoglobinases falcipain 2/2' and 3 (11–13), and a family of proteases that were termed serine repeat antigens (SERAs) (14–16). Members of this distinct *Plasmodium* protease family are clustered on chromosome II (17) and belong to papain-like cysteine proteases based on a central ~30-kD protease domain. Reverse genetics showed that some members are vital for erythrocytic schizogony, whereas others are dispensable for asexual growth *of Plasmodium* (16). However, so far no function in parasite egress has been assigned to any of these proteins. We reasoned that inactivation of a member of the *Plasmodium* papain-like cysteine protease family for which expression is restricted to sporogenic stages might lead to an essential function that can be analyzed on the cellular level. Here, we show targeted disruption of an oocyst-specific papain-like cysteine protease in *P. berghei*. Mutant sporozoites fail to egress from midgut oocysts. Therefore, we termed the corresponding protein egress cysteine protease 1 (ECP1).

The online version of this article contains supplemental material.

RESULTS AND DISCUSSION

Identification of a stage-specific *Plasmodium* cysteine protease

Several members of papain-like cysteine proteases, also termed SERAs, were previously re-

JEM © The Rockefeller University Press $8.00
Vol. 202, No. 2, July 18, 2005 225–230 www.jem.org/cgi/doi/10.1084/jem.20050545

ported to be nonessential during asexual blood-stage development (16). We tested expression of the five cysteine proteases of the *P. berghei SERA* locus by RT-PCR (Fig. 1 A). Our analysis revealed that one member (*ECP1*) displayed an interesting restriction of gene transcription to sporozoite stages. Notably, *ECP1* transcription is specific for mature oocysts, the stage that marks the final step of sporozoite generation, and is subsequently down-regulated in mature salivary gland sporozoites that are transmitted to the mammalian host (Fig. 1 B). The orthologous genes in *P. falciparum* (SERA8; PFB0325c) (17) and *P. yoelii* (PY02063) (18) show 54 and 81% overall amino acid sequence identity with *P. berghei* ECP1 (PbECP1; DQ000976), respectively (Fig. 1 C). In good agreement with our findings, the *P. falciparum* orthologue was reported recently to be expressed specifically in sporozoites (19) and absent from erythrocytic stages (20). All *Plasmodium* ECP1 proteins contain a central ~250–amino acid papain-family cysteine protease domain (Fig. 1 C). Within the domain, conservation to PbECP1 is 70% and 93% for the *P. falciparum* and *P. yoelii* orthologues, respectively. A hallmark of papain-family cysteine proteases is the presence of the catalytic triad with invariant cysteine, histidine, and asparagine residues and the oxyanion-hole glutamine residue (8). Presence of these residues in the ECP1 proteins indicates that they might function as proteases (Fig. 1 D).

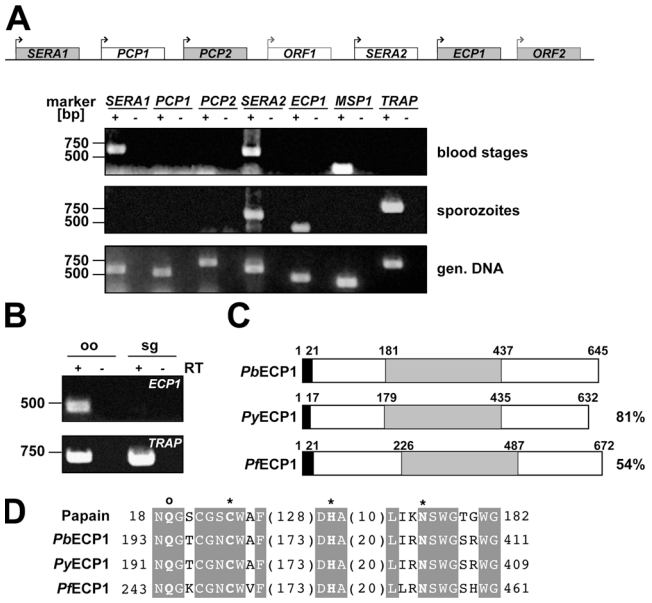

Figure 1. A stage-specific *Plasmodium* papain-like cysteine protease. (A) Expression profiling of the *P. berghei SERA* locus. (Top) Schematic diagram of the 33.5-kb *PbSERA* locus. Genes conserved between all *Plasmodium* species are shaded gray. Rodent *Plasmodium*-specific genes are in white. ECP1, egress cysteine protease 1; *PCP*, papain-like cysteine protease with an active site cysteine; *SERA*, papain-like cysteine protease with an active site serine; *ORF*, open reading frame without homology to cysteine proteases. (Bottom) RT-PCRs from mixed blood-stage and mixed sporozoite cDNAs and genomic DNA. The merozoite- and sporozoite-specific transcripts, *MSP1* and *TRAP*, were added as controls. (B) Oocyst-specific transcription of *PbECP1*. Shown is a RT-PCR analysis of *PbECP1* mRNA in oocyst sporozoites (oo) and salivary gland sporozoites (sg). (C) Primary structure of *Plasmodium* ECP1 proteins. The putative cleavable signal sequences and the central papain-like cysteine protease domains are boxed in black and gray, respectively. Overall amino acid sequence identities of the *P. yoelii* and *P. falciparum* ECP1 orthologues (PY02063 and PFB0325c, respectively) are indicated as percentage of identical residues compared with the *P. berghei* sequence. (D) Conservation of the catalytic residues of the papain family within the central cysteine protease domain. The catalytic residues (in a shaded background and marked with an asterisk) are the amino-terminal cysteine and the carboxy-terminal histidine together with the asparagine, which orients the histidine imidazole ring. The glutamine (bold and marked with 'o') in proximity to the catalytic cysteine assists in formation of the oxyanion hole. Strictly conserved amino acid residues are boxed in gray.

PbECP1 gene disruption

To study the role of *PbECP1*, we generated a loss-of-function parasite line. The endogenous *ECP1* copy was targeted with an insertion plasmid (21). Homologous recombination was expected to lead to gene disruption by generation of two truncated nontranscribed *ecp1* copies (Fig. 2 A). This strategy allows gene disruption without loss of genetic information and is likely to minimize cis effects on neighboring genes. The parental blood-stage population from the successful transfection was used for cloning three independent disruption parasite lines, termed *ecp1(-)*. Insertion-specific PCR analysis confirmed the correct insertion at the predicted locus (Fig. 2 B). To verify *PbECP1* deficiency of the mutant parasites, we performed RT-PCR and cDNA amplification using polyA$^+$ RNA from oocyst sporozoites as templates (Fig. 2 C). We also confirmed that expression of the neighboring genes, *SERA2* and *ORF2*, is not affected in the *ecp1(-)* disruptants. We next examined the phenotype of *ecp1(-)* parasites during the *Plasmodium* life cycle. As expected, *ecp1*(-) clones were indistinguishable from WT parasites in development and growth of asexual and sexual *Plasmodium* stages (unpublished data). Transmission to *Anopheles* mosquitoes and oocyst development were normal when compared with WT parasites (Table S1, available at http://www.jem.org/cgi/content/full/jem.20050545/DC1).

We next analyzed sporozoite development by examining oocyst morphology and comparing oocyst sporozoite numbers in WT and *ecp1(-)* parasites. No differences in generation of viable sporozoites were observed. Importantly, when the *ecp1*(-) sporozoites were liberated from dissected midgut oocysts, they showed the typical short residual gliding motility of WT oocyst sporozoites in vitro (Fig. 3 A). Together, our findings show that *ECP1* is dispensable for *Plasmodium* cellular functions before sporozoite release. We conclude that *ecp1(-)* parasites form viable sporozoites in numbers comparable with WT parasites, in good agreement with our observation that *ECP1* is developmentally up-regulated in mature oocysts (Fig. 1 A).

ecp1(-) sporozoites fail to egress from midgut oocysts

Upon closer examination by phase-contrast microscopy, we observed a peculiar arrangement of sporozoites within the

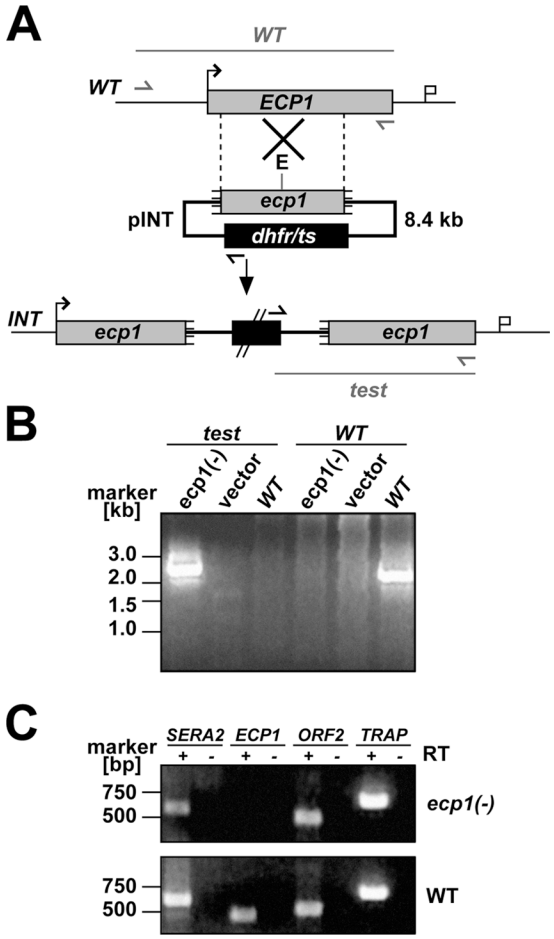

Figure 2. Targeted gene disruption of *P. berghei ECP1*. (A) Insertion strategy to generate the *ecp1(-)* parasites. The WT *ECP1* genomic locus (*WT*) is targeted with an *EcoRV* (E)-linearized integration plasmid (pINT) containing 5′ and 3′ truncations of the *ECP1* open reading frame and the *dhfr/ts* positive selectable marker. Upon a single crossover event, the region of homology is duplicated, resulting in two truncated, nonexpressed *ecp1* copies in the recombinant locus (*INT*). Integration-specific test and WT primer combinations are indicated by arrows and expected fragments as lines. (B) Integration-specific PCR analysis. The successful integration event is verified by a primer combination (test) that can amplify only a signal from the *INT* locus. Absence of the WT signal from *ecp1(-)* parasites confirms the purity of the clonal population. (C) Absence of *ECP1* transcripts in *ecp1(-)* parasites. cDNA from WT and *ecp1(-)* oocyst sporozoites were amplified in the presence (+) or absence (-) of reverse transcriptase (RT). Note that expression of the adjacent genes, *SERA2* and *ORF2* (Fig. 1 A), are not affected in the *ecp1(-)* parasites.

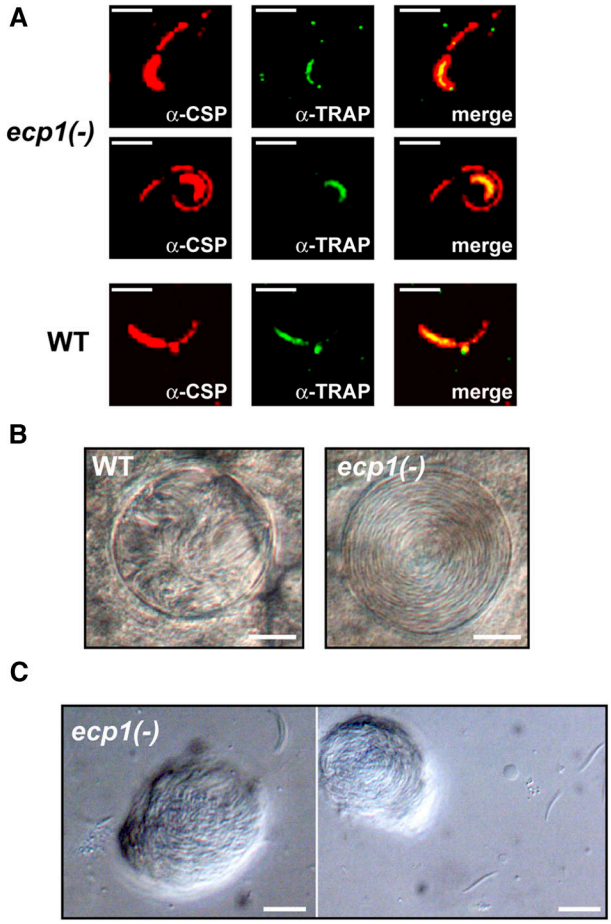

Figure 3. *ecp1(-)* oocysts generate viable sporozoites. (A) *ecp1(-)* oocyst sporozoites display normal gliding locomotion. Shown are representative immunofluorescence stainings of *ecp1(-)* and WT oocyst sporozoites with anti-PbCSP antibodies (28) and anti-TRAP antisera (29). Gliding sporozoites deposit CSP in their trails. Bars, 10 μm. (B) *ecp1(-)* sporozoites are confined within oocysts. Shown are interference contrast micrographs of WT and *ecp1(-)* oocysts. WT sporozoites are arranged radially and will eventually exit the oocyst. In contrast, *ecp1(-)* sporozoites do not escape the oocysts and orient in circles under continuous gliding locomotion (Video 1). Bars, 10 μm. (C) Sporozoite clusters from *ecp1(-)*-infected mosquitoes. Shown are micrographs from isolated and ground midguts. Free sporozoite clusters can be detected in the dissection medium indicating that lack of *ECP1* alters the normal oocyst rupturing process. Bars, 10 μm.

oocysts (Fig. 3 B). Although WT sporozoites are arranged in a radial fashion, *ecp1(-)* sporozoites seemed to be organized in circles. Intriguingly, *ecp1(-)* sporozoites displayed a continuous circular movement around a central axis, in both clockwise and anticlockwise directions (Video 1, available at http://www.jem.org/cgi/content/full/jem.20050545/DC1). In WT oocysts, sporozoite bending and flexing is seen on rare occasions, presumably in preparation for egress from the oocyst (unpublished data). In general, no motility can be observed in WT oocysts (Video 2, available at http://www.jem.org/cgi/content/full/jem.20050545/DC1). In marked contrast, continuous circular motility was observed in all *ecp1(-)* oocysts examined. This previously unrecognized motility within midgut oocysts is likely a consequence of a defect after completion of sporogony. This observation prompted us to perform a detailed spatial and temporal analysis of sporozoite distribution within the *Anopheles* mosquito (Table I). Intriguingly, no sporozoites were detected in the hemocoel or in the salivary glands of infected mosquitoes despite efficient infection rates and high numbers of oocyst sporozoites. Although we continued to look for salivary

Table I. *ecp1(-)* parasites are deficient in exiting midgut oocysts

	ecp1(-) sporozoites[a]			WT sporozoites[a]		
Days[b]	Oocyst	Hemocoel	Salivary gland	Oocyst	Hemocoel	Salivary gland
12–14	78,200 (5)	ND	ND	55,500 (5)	ND	ND
15	82,290 (9)	0 (3)	0 (3)	41,314 (11)	627 (3)	7,220 (5)
18	111,333 (6)	ND	0 (5)	36,880 (5)	ND	15,440 (5)
20–28	115,750 (6)	0 (2)	0 (6)	13,045 (4)	200 (2)	10,100 (3)
30–40	108,000 (5)	ND	0 (3)	6,175 (4)	ND	10,633 (3)
50–55	38,500 (2)	ND	0 (2)	40 (2)	ND	ND

[a]Mean number of sporozoites per infected mosquito in the respective tissue. Numbers of independent feeding experiments are shown in parentheses.
[b]Time point of dissection after feeding.

gland sporozoites throughout the life span of the mosquitoes (~55 d after feeding) we failed to detect *ecp1*(-) salivary gland sporozoites. In WT parasites, oocyst sporozoite numbers peak at ~day 14 after infection. Thereafter, sporozoites are released continuously into the hemocoel, where they can be detected transiently (Table I). Sporozoites enter salivary glands rapidly and actively; their final destination in the invertebrate host (22). Accordingly, numbers of oocyst sporozoites decline over time, whereas salivary glands remain filled with sporozoites, rendering infected mosquitoes infectious for life. In striking contrast, *ecp1(-)* oocysts do not rupture, resulting in a remarkable accumulation of viable sporozoites (Table I). Hence, the observed intraoocyst motility is likely a consequence of the failure to egress the oocysts. We also noticed that none of the persisting *ecp1(-)* oocysts was melanized throughout the mosquito life span, nor were the survival rates of the infected mosquitoes affected (unpublished data). Together, our data indicate that oocysts are not breached passively by parasite growth. Instead, we propose that sporozoite egress is an active process that requires *ECP1* functions.

Next, we tested whether viable motile *ecp1(-)* oocyst sporozoites are infectious to the mammalian host. We injected highly susceptible Sprague/Dawley rats with either WT or *ecp1(-)* oocyst sporozoites (Table S2, available at http://www.jem.org/cgi/content/full/jem.20050545/DC1). As expected, we achieved consistent blood-stage infections with 100,000 WT oocyst sporozoites. In striking contrast, animals injected with even 10-fold higher doses of *ecp1(-)* sporozoites remained malaria free, suggesting additional functions of *ECP1* after oocyst rupture.

Lack of *ECP1* results in protected oocysts

Upon midgut dissection we also observed that *ecp1*(-) oocysts were resistant to light mechanical stress such as gentle grinding to free sporozoites. Occasionally we detected free-floating oocysts that were detached from the midgut (Fig. 3 C). The oocyst capsule has a bipartite structure with the inner layer being of parasite origin and the outer thick layer deriving from the basal lamina of the mosquito midgut (23). The inner oocyst membrane is covered by the circumsporozoite protein (CSP) (24) and, hence, can serve as a marker for oocyst permeabilization. To test if *ecp1(-)* oocysts are more rigid than WT oocysts, we dissected midguts and permeabilized oocysts with the detergent saponin (Fig. 4 A). Although all oocysts can be permeabilized with methanol and displayed strong circumferential CSP staining, only WT oocysts could be permeabilized by the natural surfactant saponin (Fig. 4 A). This finding suggests that developing *Plasmodium* oocysts are protected by an impermeable oocyst wall that is processed actively after sporozoite maturation. To control for CSP levels in *ecp1(-)* oocyst sporozoites, we performed a Western blot analysis of sporozoites dissected in the absence or presence of the cysteine protease inhibitor E64 (Fig. 4 B; reference 25). We detected a previously unrecognized additional CSP band that was specific for oocyst sporozoites. Notably, this signal was abundant only in the *ecp1(-)* mutant or when WT midguts were dissected in the presence of E64. These findings may indicate a role of ECP1 in CSP processing. Although the substrate of ECP1 is not known yet, CSP is a likely candidate for a direct or indirect

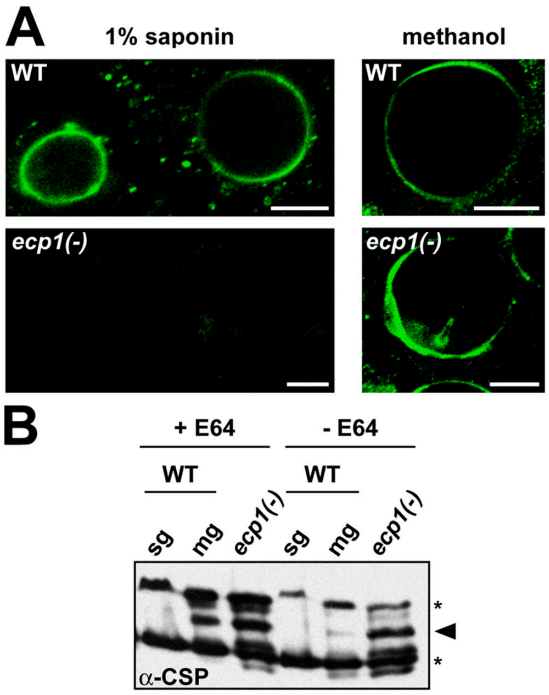

Figure 4. Oocysts are protected in *ecp1(-)* parasites. (A) *ecp1(-)* oocysts are resistant to permeabilization by detergents (1% saponin). The inner oocyst membrane is stained with highly diluted anti-PbCSP antibody (1:1,000). Proper CSP localization is shown in methanol-fixed oocysts. Bars, 10 μm. (B) Western blot analysis of CSP in isolated salivary gland (sg) or midgut (mg) sporozoites from WT or midgut sporozoites from *ecp1(-)* parasites. In addition to the typical CSP doublet (marked with asterisks), an intermediate midgut-specific band can be detected in the *ecp1(-)* mutant and in WT sporozoites that were isolated in the presence of 100 μM cysteine protease inhibitor E64.

downstream proteolytic processing event, particularly because it seems to be one of the dominant parasite-derived components lining the inner side of the oocysts (24).

Collectively, our data suggest that *ECP1* plays a central role in the egress of the sporozoites from midgut oocysts. Lack of ECP1 proteolytic activity blocked the life cycle of malaria parasites inside the mosquito vector at the oocyst stage. Therefore, inhibition of oocyst rupture provides an additional target for transmission-blocking strategies. Oocysts stand out in the *Plasmodium* life cycle, because they represent the longest developmental phase and the only replicative phase of the malaria parasites that does not need host cells for its expansion. Despite their importance, oocysts remain the least-characterized mosquito stage of *Plasmodium*. Purification of protected *ecp1(-)* oocysts may provide a rare resource for a detailed analysis of the molecular repertoire of mature oocysts. Our study may pave the way for the identification of similar egress cysteine proteases that drive merozoite release from liver-stage and blood-stage schizonts by targeted gene disruption. This possibility is supported by the inhibitory effect of cysteine protease inhibitors on merozoite egress from host erythrocytes (5, 6). Identifying an essential function of cysteine proteases, such as the one of *ECP1* for sporozoite egress, is fundamental for drug-target validation and rational design of inhibitors.

MATERIALS AND METHODS

Experimental animals. Animals were from Charles River Laboratories. All animal work was conducted in accordance with European regulations and approved by the state authorities (Regierungspräsidium Karlsruhe).

Generation of the *ecp1(-)* parasite line. For targeted disruption of *ECP1*, an integration vector was generated by amplification of a PCR fragment using *P. berghei* genomic DNA as template and primers ECP1for (5′-GGACTAGTGAGCATATAGAAAGCCATATTCAAC-3′; SpeI site is underlined) and ECP1rev (5′-TCCCCGCGGGCACC-TTGCTCAATTATGTAATCTTTTAAG-3′; *Sac*II site is underlined). Cloning into the *P. berghei* transfection vector (21) resulted in plasmid pAA05. The targeting plasmid was linearized with EcoRV, and parasite transfection, positive selection, and parasite cloning were performed as described previously (21). Integration-specific PCR amplification of the *ecp1(-)* locus was generated using specific primer combinations. We obtained three independent *ecp1(-)* clonal parasite populations that were phenotypically identical. Detailed analysis was performed with one representative clone.

Transcript detection. For RT-PCR analysis, we isolated poly (A^+) RNA from 5×10^5 WT salivary gland sporozoites and 10^6 WT and *ecp1(-)* oocyst sporozoites, respectively, using oligo dT-columns (Invitrogen). For cDNA synthesis and amplification, we performed a two-step PCR using random decamer primers (Ambion) and subsequent standard PCR reactions, using gene-specific primers.

Phenotypical analysis during the *Plasmodium* life cycle. Blood-stage development was analyzed in vivo in asynchronous infections using Naval Medical Research Institute mice. Gametocyte differentiation and exflagellation of microgametes were detected in mice before mosquito feedings. Sporozoite populations were separated and analyzed as described previously (26, 27). Adherent sporozoites were incubated with a mAb against *P. berghei* circumsporozoite protein (PbCSP) (28) and a polyclonal anti–*P. berghei* thrombospondin-related anonymous protein (TRAP) antiserum (29). Bound antibodies were detected using Alexa Fluor 546–conjugated anti–mouse antibodies and Alexa Fluor 488–conjugated anti–rabbit antibodies, respectively (Molecular Probes).

In vivo infectivity of sporozoites. For determination of the infectivity of oocyst sporozoites, infected midguts were dissected at days 15–17 after feeding. Sporozoites were liberated and injected i.v. at the numbers indicated into young Sprague/Dawley rats. Patency was checked daily by Giemsa-stained blood smears.

Oocyst immunofluorescence. For the analysis of CSP localization in the oocysts, infected midguts were fixed in 2% formaldehyde/0.2% glutaraldehyde, permeabilized with 1% saponin in PBS/1% FCS or with ice-cold methanol and incubated with primary anti-PbCSP (1:1,000; reference 28). At the high-antibody dilution, internal sporozoites are not visualized. Bound antibodies were detected using Alexa Fluor 488–conjugated anti–mouse antibodies.

Western blot analysis. For detection of CSP levels in WT and *ecp1(-)* oocysts, we dissected midguts of infected mosquitoes at day 15 after infection. Infected midguts were isolated, ground, and pelleted in the presence or absence of freshly prepared 100-μM E64 (Sigma-Aldrich; reference 5). Total oocyst lysates equivalent to 100,000 oocyst sporozoites and, as a control, 100,000 WT salivary gland sporozoites were separated on a 10% SDS PAGE and transferred to a nitrocellulose membrane. CSP was detected with primary anti-PbCSP (1:8,000; reference 28). Bound antibodies were detected using horseradish peroxidase–conjugated anti-mouse antibodies (Sigma-Aldrich).

Online supplemental material. Table S1 shows that oocyst development of *ecp1(-)* parasites is not affected compared with WT parasites. Table S2 shows that *ecp1(-)* oocyst sporozoites are noninfectious to the mammalian host. Video 1 shows real-time live-imaging of *ecp1(-)* oocysts. *ecp1(-)* sporozoites lack the capacity to egress oocysts and instead display continuous circular motility. Video 2 shows the corresponding WT oocysts with no detectable internal motility. Online supplemental material is available at http://www.jem.org/cgi/content/full/jem.20050545/DC1.

We gratefully acknowledge A. Kunze for expert technical assistance and A. Baumm and R. Mosbach for professional help with the video documentation. We are grateful to Dr. V. Nussenzweig for sharing unpublished results and critically reviewing the text.

Our work was supported by grants from the research focus "Tropical Medicine Heidelberg" of the Medical Faculty of Heidelberg University and the European Commission (BioMalPar 23).

The authors have no conflicting financial interests.

Submitted: 14 March 2005
Accepted: 14 June 2005

REFERENCES

1. Sibley, L.D. 2004. Intracellular parasite invasion strategies. *Science*. 304: 248–253.
2. Blackman, M.J. 2000. Proteases involved in erythrocyte invasion by the malaria parasite: function and potential as chemotherapeutic targets. *Curr. Drug Targets*. 1:59–83.
3. Hadley, T., M. Aikawa, and L.H. Miller. 1983. *Plasmodium knowlesi*: studies on invasion of rhesus erythrocytes by merozoites in the presence of protease inhibitors. *Exp. Parasitol*. 55:306–311.
4. Lyon, J.A., and J.D. Haynes. 1986. *Plasmodium falciparum* antigens synthesized by schizonts and stabilized at the merozoite surface when schizonts mature in the presence of protease inhibitors. *J. Immunol*. 136:2245–2251.
5. Salmon, B.L., A. Oksman, and D.E. Goldberg. 2001. Malaria parasite exit from the host erythrocyte: a two-step process requiring extraerythrocytic proteolysis. *Proc. Natl. Acad. Sci. USA*. 98:271–276.
6. Wickham, M.E., J.G. Culvenor, and A.F. Cowman. 2003. Selective inhibition of a two-step egress of malaria parasites from the host eryth-

rocyte. *J. Biol. Chem.* 278:37658–37663.
7. Rosenthal, P.J., K. Kim, J.H. McKerrow, and J.H. Leech. 1987. Identification of three stage-specific proteinases of *Plasmodium falciparum*. *J. Exp. Med.* 166:816–821.
8. Rosenthal, P.J. 2004. Cysteine proteases of malaria parasites. *Int. J. Parasitol.* 34:1489–1499.
9. Sijwali, P.S., K. Kato, K.B. Seydel, J. Gut, J. Lehman, M. Klemba, D.E. Goldberg, L.H. Miller, and P.J. Rosenthal. 2004. *Plasmodium falciparum* cysteine protease falcipain-1 is not essential in erythrocytic stage malaria parasites. *Proc. Natl. Acad. Sci. USA.* 101: 8721-8726.
10. Eksi, S., B. Czesny, D.C. Greenbaum, M. Bogyo, and K.C. Williamson. 2004. Targeted disruption of *Plasmodium falciparum* cysteine protease, falcipain 1, reduces oocyst production, not erythrocytic growth. *Mol. Microbiol.* 53:243–250.
11. Shenai, B.R., P.S. Sijwali, A. Singh, and P.J. Rosenthal. 2000. Characterization of native and recombinant falcipain-2, a principal trophozoite cysteine protease and essential hemoglobinase of *Plasmodium falciparum*. *J. Biol. Chem.* 275:29000–29010.
12. Sijwali, P.S., B.R. Shenai, J. Gut, A. Singh, and P.J. Rosenthal. 2001. Expression and characterization of the *Plasmodium falciparum* hemoglobinase falcipain-3. *Biochem. J.* 360:481–489.
13. Sijwali, P.S., and P.J. Rosenthal. 2004. Gene disruption confirms a critical role for the cysteine protease falcipain-2 in hemoglobin hydrolysis by *Plasmodium falciparum*. *Proc. Natl. Acad. Sci. USA.* 101:4384–4389.
14. Delplace, P., J.-F. Dubremetz, B. Fortier, and A. Vernes. 1985. A 50 kilodalton exoantigen specific to the merozoite release-reinvasion stage of *Plasmodium falciparum*. *Mol. Biochem. Parasitol.* 17:239–251.
15. Bzik, D.J., W.-b. Li, T. Horii, and J. Inselburg. 1988. Amino acid sequence of the serine-repeat antigen (SERA) of *Plasmodium falciparum* determined from cloned cDNA. *Mol. Biochem. Parasitol.* 30:279–288.
16. Miller, S.K., R.T. Good, D.R. Drew, M. Delorenzi, P.R. Sanders, A.N. Hodder, T.P. Speed, A.F. Cowman, T.F. de Koning-Ward, and B.S. Crabb. 2002. A subset of *Plasmodium falciparum* SERA genes are expressed and appear to play an important role in the erythrocytic cycle. *J. Biol. Chem.* 277:47524–47532.
17. Gardner, M.J., H. Tettelin, D.J. Carucci, L.M. Cummings, L. Aravind, E.V. Koonin, S. Shallom, T. Mason, K. Yu, C. Fujii, et al. 1998. Chromosome 2 sequence of the human malaria parasite *Plasmodium falciparum*. *Science.* 282:1126–1132.
18. Carlton, J.M., S.V. Angiuoli, B.B. Suh, T.W. Kooij, M. Pertea, J.C. Silva, M.D. Ermolaeva, J.E. Allen, J.D. Selengut, H.L. Koo, et al. 2002. Genome sequence and comparative analysis of the model rodent malaria parasite *Plasmodium yoelii yoelii*. *Nature.* 419:512–519.
19. LeRoch, K.G., Y. Zhou, P.L. Blair, M. Grainger, J.K. Moch, J.D. Haynes, P. De La Vega, A.A. Holder, S. Batalov, D.J. Carucci, and E.A. Winzeler. 2003. Discovery of gene function by expression profiling of the malaria life cycle. *Science.* 301:1503–1508.
20. Bozdech, Z., M. Llinas, B.L. Pulliam, E.D. Wong, J. Zhu, and J.L. DeRisi. 2003. The transcriptome of the intraerythrocytic developmental cycle of *Plasmodium falciparum*. *PloS Biol.* 1:85–100.
21. Thathy, V., and R. Ménard. 2002. Gene targeting in *Plasmodium berghei*. *Methods Mol. Med.* 72:317–331.
22. Kappe, S.H.I., K. Kaiser, and K. Matuschewski. 2003. The *Plasmodium* sporozoite journey: a rite of passage. *Trends Parasitol.* 19:135–143.
23. Sinden, R.E. 2002. Molecular interactions between *Plasmodium* and its insect vectors. *Cell. Microbiol.* 4:713–724.
24. Thathy, V., H. Fujioka, S. Gantt, R. Nussenzweig, V. Nussenzweig, and R. Ménard. 2002. Levels of circumsporozoite protein in the *Plasmodium* oocyst determine sporozoite morphology. *EMBO J.* 21:1586–1596.
25. Coppi, A., C. Pinzon-Ortis, C. Hutter, and P. Sinnis. 2005. The *Plasmodium* circumsporozoite protein is proteolytically processed during cell invasion. *J. Exp. Med.* 201:27–33.
26. Vanderberg, J.P. 1974. Studies on the motility of *Plasmodium* sporozoites. *J. Protozool.* 21:527–537.
27. Vanderberg, J.P. 1975. Development of infectivity by the *Plasmodium berghei* sporozoite. *J. Parasitol.* 61:43–50.
28. Potocnjak, P., N. Yoshida, R.S. Nussenzweig, and V. Nussenzweig. 1980. Monovalent fragments (Fab) of monoclonal antibodies to a sporozoite surface antigen (Pb44) protect mice against malarial infection. *J. Exp. Med.* 151:1504–1513.
29. Sultan, A.A., V. Thathy, U. Frevert, K.J. Robson, A. Crisanti, V. Nussenzweig, R.S. Nussenzweig, and R. Ménard. 1997. TRAP is necessary for gliding motility and infectivity of *Plasmodium* sporozoites. *Cell.* 90:511–522.